Since January 2020 Elsevier has created a COVID-19 resource centre with free information in English and Mandarin on the novel coronavirus COVID-19. The COVID-19 resource centre is hosted on Elsevier Connect, the company's public news and information website.

Elsevier hereby grants permission to make all its COVID-19-related research that is available on the COVID-19 resource centre - including this research content - immediately available in PubMed Central and other publicly funded repositories, such as the WHO COVID database with rights for unrestricted research re-use and analyses in any form or by any means with acknowledgement of the original source. These permissions are granted for free by Elsevier for as long as the COVID-19 resource centre remains active.

Virus Research 294 (2021) 198275

Contents lists available at ScienceDirect

Virus Research

journal homepage: www.elsevier.com/locate/virusres

Tmprss2 specific miRNAs as promising regulators for SARS-CoV-2 entry checkpoint

Taruneet Kaur [a,**], Suman Kapila [a], Rajeev Kapila [a,1], Sandeep Kumar [b], Divya Upadhyay [a], Manjeet Kaur [c], Chandresh Sharma [d,*]

[a] Animal Biochemistry Division, ICAR-National Dairy Research Institute, Karnal, Haryana, 132001, India
[b] Virus Research and Diagnostic Laboratory, Kalpana Chawla Government Medical College, Karnal, Haryana, 132001, India
[c] Centre for Agricultural Bioinformatics, ICAR-Indian Agricultural Statistics Research Institute, New Delhi, 110012, India
[d] Multidisciplinary Clinical Translational Research, Translational Health Science and Technology Institute, Faridabad, Haryana, 121001, India

ARTICLE INFO

Keywords:
COVID-19
hsa-miR-214
hsa-miR-98
hsa-miR-32
Tmprss2

ABSTRACT

Tmprss2 is an emerging molecular target which guides cellular infections of SARS-CoV-2, has been earmarked for interventions against the viral pathologies. The study aims to computationally screen and identifies potential miRNAs, following *in vitro* experimental validation of miRNA-mediated suppression of Tmprss2 for early prevention of COVID-19. Pool of 163 miRNAs, scrutinized for Tmprss2 binding with three miRNA prediction algorithms, ensued 11 common miRNAs. Further, computational negative energies for association, corroborated miRNA-Tmprss2 interactions, whereas three miRNAs (hsa-miR-214, hsa-miR-98 and hsa-miR-32) based on probability scores ≥0.8 and accessibility to Tmprss2 target have been selected in the Sfold tool. Transfection of miRNA(s) in the Caco-2 cells, quantitatively estimated differential expression, confirming silencing of Tmprss2 with maximum gene suppression by hsa-miR-32 employing novel promising role in CoV-2 pathogenesis. The exalted binding of miRNAs to Tmprss2 and suppression of later advocates their utility as molecular tools for prevention of SARS-CoV-2 viral transmission and replication in humans.

1. Introduction

Recent human pandemics worldwide, including south-east Asia, have been linked to the emergence of a novel Severe Acute Respiratory Syndrome CoronaVirus 2 (SARS-CoV-2 or CoV-2), at the end of 2019 in Wuhan, China, causing CoronaVirus Disease 2019 (COVID-19). SARS-CoV-2 is an enveloped RNA virus and has been classified as a subfamily of Orthocoronavirinae, with similarities of 79.5 % and 96 % of SARS-CoV and Bat coronavirus respectively (Zhou et al., 2020). Its entry in the host, is majorly assisted by viral spike (S) protein, relying chiefly on contacts among S1 unit (S protein) with the target receptor (ACE2) (Verdecchia et al., 2020). Besides, cleavage of S protein (spike protein) by a transmembrane serine protease (Tmprss2), is the next step for viral invasion generating both S1 and S2 units. In order to blend host and viral membranes, the cleavage step is critical and ultimately results in viral entry (Hoffmann et al., 2020). In the human metapneumovirus activation process, Tmprss2 was also documented (Shirogane et al., 2008). Furthermore, it was shown that another Tmprss11a protein enhances the virulence of the SARS's S protein and helps its degradation. (Shirogane et al., 2008). Moreover, the stimulating ability of human influenza viruses in type II Tmprss2 and Tmprss4 has been demonstrated (Kuhn et al., 2016; Matsuyama et al., 2010). In a Tmprss2 knockout mouse model, the infectivity for H1N1 influenza and the symptoms associated are attenuated (Tarnow et al., 2014). As Tmprss2 has an important and evident role in the pathogenesis and expansion of CoV-2, it may be useful for therapeutically promising strategies targeted at Tmprss2 expression in the host (human). Currently, inhibitory drug *viz.* camostat mesylate demonstrated great therapeutic potential against CoV-2 in the enzymatic suppression of Tmprss2 (Bittmann et al., 2020) with experimental confirmation using Caco-2 and Vero cells (Hoffmann et al., 2020). However, it is associated with major toxicity concerns with observed oedema and urticaria at higher doses (Uno, 2020). In the last

* Corresponding author at: Translational Health Science and Technology Institute, (An autonomous institute of the Department of Biotechnology, Government of India), NCR Biotech Science Cluster, 3rd Milestone, Faridabad–Gurugram Expressway, PO box #04, Faridabad, Haryana.
** Co-corresponding author at: Animal Biochemistry Division, National Dairy Research Institute, Karnal, Haryana, 132001, India.
E-mail addresses: taruk04@gmail.com (T. Kaur), chandresh@thsti.res.in (C. Sharma).
[1] https://www.researchgate.net/profile/Rajeev_Kapila5.

https://doi.org/10.1016/j.virusres.2020.198275
Received 17 September 2020; Received in revised form 27 November 2020; Accepted 17 December 2020
Available online 8 January 2021
0168-1702/© 2020 Elsevier B.V. All rights reserved.

two decades, microRNAs (miRNAs) have emerged as a molecular tool in the post-transcriptional modulation of the essential regulatory molecules in the cellular micro-environment (Filipowicz et al., 2008). miRNAs are antisense, short (21–23 nucleotides) RNA molecules, targeting mRNAs (3′UTR) and protein translational processes (Gu et al., 2009). Anti CoV-2 therapeutic interventions with approved small molecules as drugs and monoclonal antibodies have been promising in the initial disease management, however, their efficacy needs to be established globally, and nevertheless, not all genes could be exploited to translate as therapeutics using such methods. While miRNAs hold immense potential in the rapid development of bio-drugs against various target genes associated with a signalling pathway (Ishida and Selaru, 2013). Moreover, miRNAs being endogenous makes them less immunogenic in nature. miRNA driven therapies, as molecular modulators, are crucially recommended for treating microbial infections, cancers and numerous disorders (Bandiera et al., 2015). Since the viral genes are translated within the host cell, endogenous miRNAs may assist in managing various replication processes associated with SARS CoV-2 and the host genome. In addition, several recent studies have demonstrated the prominence of miRNA function and dysfunction, targeting mRNA transcripts that are present in the CoV-2 genome. Recently, hsa-miR101 has been documented targeting the viral NSP (nonstructural protein), which is an established crucial therapeutics (Sardar et al., 2020). Likewise, Zoni et al., reported miR182 with a potential function to regulate TMPRSS2-ERG interactions in prostate cancer (Zoni et al., 2018). In the miRNAs-based therapies, miRNAs need to bind their cognate mRNA targets with high affinity and least off-target effects. Given prediction of precise miRNA targets, numerous computational tools are available (Peterson et al., 2014). Therefore, in the present study, an *in silico* pipeline was used to identify three highly specific potent human miRNAs along with their *in vitro* experimental validations in the human colorectal adenocarcinoma cell line; Caco-2, representing an illustrious binding to the Tmprss2, which ultimately may be exploited to design miRNA-based bio-drug therapeutics to repress Tmprss2, tends to the consequent control of COVID-19 infection in human.

2. Material and methods

2.1. Chemicals

Human colorectal adenocarcinoma cell line-Caco-2 (National Centre for Cell Science, Pune, India). Penicillin, streptomycin, amphotericin, Dulbecco's modified Eagle's medium (DMEM), Fetal Bovine Serum (FBS), L-glutamine (Sigma, St. Louise, M.O., USA). mirVana miRNA isolation kit, lipofectamine RNAiMAX (Thermo Scientific, Waltham, MA, USA). Hsa-miR-214/ miR214, hsa-miR-98/ miR98 and hsa-miR-32-3p/ miR32 mimics and negative control (miC) (Ambion, Applied Biosystems, Foster City, CA, USA). Plastic dishes and culture plates (Corning, NY, USA).

2.2. Gene sequence collection

The work scheme followed in this study is illustrated in Fig. 1, the 3′UTR (Untranslated regions) sequence of human Tmprss2 (Homo sapiens transmembrane serine protease 2, transcript variant 2, mRNA, RefSeq NM_005656) was acquired from NCBI database (www.ncbi.nlm.nih.gov), Gencode Transcript: ENST00000332149.10, Gencode Gene: ENSG00000184012.12, Position: hg38 chr21:41,464,305-41,508,158. It's a linear mRNA and 3′UTR sequence is 1837 nucleotides in length.

2.3. miRNA prediction tools and selection criteria

The prediction for miRNA(s) was executed using three different *in silico* tools *viz.* miRDB (http://mirdb.org/), TargetScan (Human, 7.2, http://www.targetscan.org/vert_72/) and miRanda (http://www.microrna.org/).The common miRNA(s) predicted by all the three prediction tools were selected for further screening, represented in the form of Venn Diagram Venny2.1, (https://bioinfogp.cnb.csic.es/tools/venny).

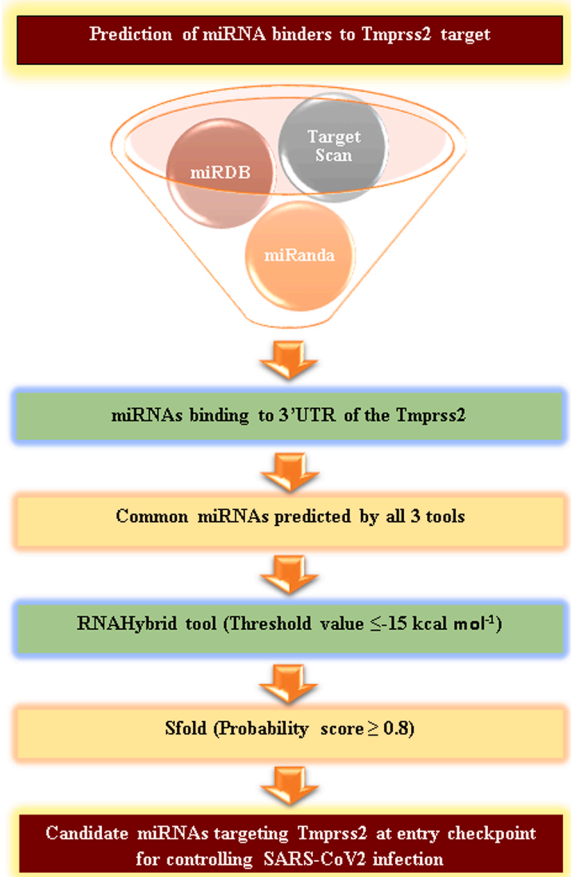

Fig. 1. Schematic representation of computational prediction pipeline for identification of the therapeutic miRNAs.

2.4. Negative energy calculations (ΔGhybrid) for miRNA-Tmprss2 hybrid

RNAHybrid tool (https://bibiserv.cebitec.uni-bielefeld.de/rnahybrid/) was employed for the negative energy calculations between the binding pair, miRNA and target (Tmprss2). In order to attain binding hybrid with high negative energies, number of hits allowed per target and threshold value for the ΔGhybrid were fixed as 5 and −15 kcal mol^{-1} respectively while human-3′UTR was selected as species filter (Rehmsmeier et al., 2004). ΔGhybrid is the stability estimate for miRNA-target hybrid by RNAhybrid; threshold value of −15 kcal mol^{-1} or lower represents greater chances of stable hybridization.

2.5. Secondary structure analysis and Target accessibility

The secondary structure prediction for the precursor miRNAs (pre-miRNA), mature miRNA and Tmprss2 was performed using RNAfold tool (http://rna.tbi.univie.ac.at/cgi-bin/RNAWebSuite/RNAfold.cgi). The *in silico* parameters were set as default. For target accessibility, Sfold web server (http://sfold.wadsworth.org/cgi-bin/index.pl) was used. Probability score, LogitProb represents confidence measure for the prediction of the accurate binding site, a score of 0.5 or higher reflects satisfactory binding possibility for the miRNA in the predicted target site. ΔGnucl displays estimate of nucleation potential for miRNA-target hybridization; for favorable nucleation ΔGN + ΔGinitiation <0 kcal mol^{-1} was considered. ΔGtotal depicts estimate for change in total energy of the hybridization; acceptable threshold −10 kcal mol^{-1} or lower.

Site_Access is the estimate for structural accessibility calculated basis average probability of unpaired nucleotides in the binding site; Upstream_AU is the AU content for the block of nucleotides upstream the binding site. Dwstream_AU is the AU content for the block of nucleotides downstream of the binding site; threshold for functional target-miRNA binding was considered as 0.6 (Ding et al., 2004; Rennie et al., 2014).

2.6. Cell culture

Caco-2 cells were allowed to grow in DMEM, containing 4500 mg L^{-1} glucose, 10 % FBS, 2 mmol/L L-glutamine and antibiotics (penicillin 100 U/mL, streptomycin 30 μg/mL, amphotericin 25 μg/mL) at 37 °C in a CO_2 incubator with 5 % CO_2.

2.7. miRNA transfection and validation

Caco-2 were primarily indorsed to accomplish 70 % confluency and further treated with Mock Control (MC), miC (negative control) and hsa-miRNA mimics (synthetic miRNA molecules) at 20, 40, 80 nM concentrations by means of RNAiMAX reagent, added in the Opti-MEM®I Reduced Serum Medium (Invitrogen, Carlsbad, CA, USA) according to the manufacturer's instructions. The transfection was continued for 6 h, and the reduced media was further replaced by DMEM, 10 % FBS and antibiotics. Finally, the cells were harvested for RNA isolation after 2 d of the transfection. MC contains transfecting Opti-MEM media with RNAiMAX transfecting reagent.

For total RNA isolation, mirVana miRNA isolation kit was used and the effective transfection for miRNA was evaluated by miScript II RT kit and miScript SYBR® Green PCR Kit (Qiagen, Madrid, Spain) in concordance with manufacture's information (Supplemental Method 1). The primer sequences for miRNA real time gene expression analysis are listed in Supplementary Table 1.

For the expression of Tmprss2 transcript, primer sequence is mentioned in Supplementary Table 1, with protocol followed as reported in previous studies (John et al., 2018).

For TMPRSS2 protein expression, transfected RCO (miC, miRNA mimic and AntimiRNA, 40 nM) were initially washed and lysed by Laemmli Lysis-buffer (Sigma). Immunoblotting procedure was executed after the lysis of the cell. TMPRSS2 and β actin Antibodies were procured from Abcam, USA. Densitometry analysis for the blots was accomplished using ImageJ (Kaur et al., 2020).

2.8. Statistical examination

Data are denoted in mean ± S.E.M. The data obtained as results in different treatment groups were subjected to one-way ANOVA based analysis, followed by Newman–Keuls test of significance by the means of GraphPad Prism software (v.8). The experiments were repeated three times with representative observations depicted in the manuscript. Resultant values with $p < 0.05$ were designated as statistically significant.

3. Results

3.1. Identification and selection of miRNAs targeting Tmprss2

Computational scanning of Tmprss2, using three different *in silico* target predication tools *viz.* miRDB, TargetScanHuman and miRanda provided 63, 30 and 30 miRNAs respectively (Figs. 2a–c). 3′UTR transcript (1837 nucleotides long) of the Tmprss2 was acquired from NCBI and only the miRNAs having high prediction scores in each of the three tools were selected and reported. The working scheme for the present investigation is illustrated in Fig.1.

3.2. Sorting of the miRNAs

The total resultant miRNAs were further filtered based on the prediction by all the three tools (Fig. 2d). Fig. 2e displays the list of miRNAs resulted from two prediction tools (TargetScanHuman 7.2 and miRDB; 17 miRNAs). Albeit, list of putative miRNAs (11 miRNAs) retrieved as result from all the three prediction tools is represented in Fig. 2f. The binding interactions of the miRNA-Tmprss2 *via*, miRanda and

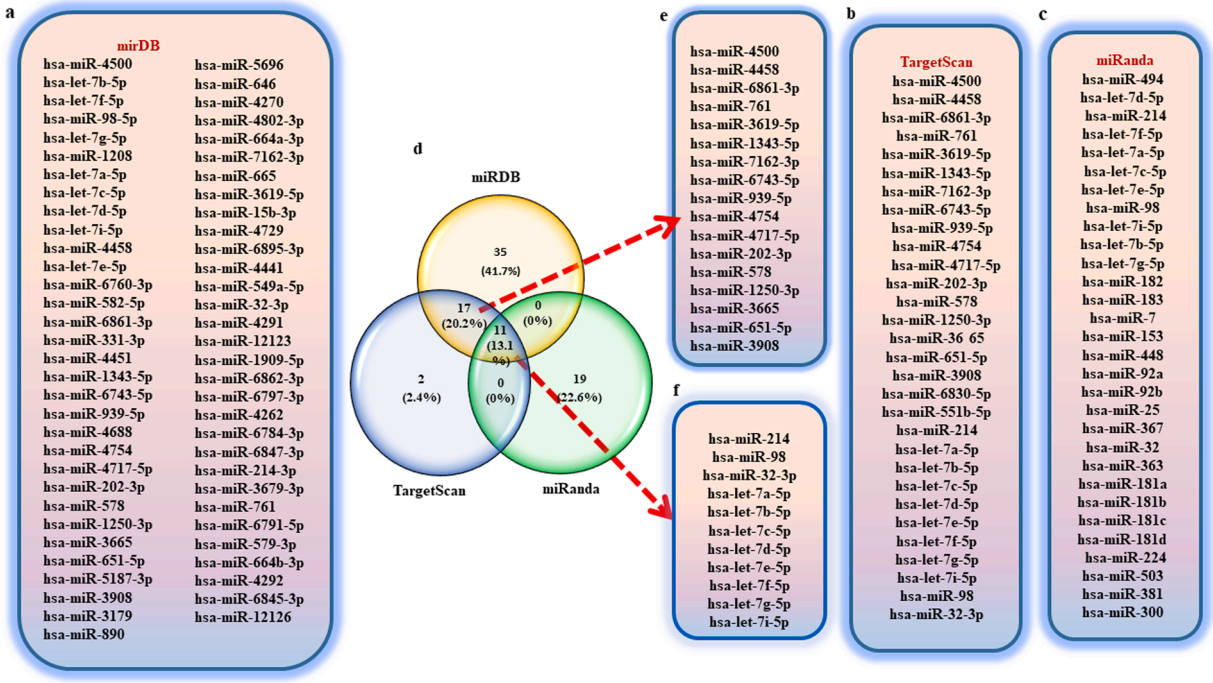

Fig. 2. Identification of miRNAs from the pool, by computational predictions targeting Tmprss2 **a.** miRNAs reported by miRDB miRNA prediction tool **b.** miRNAs reported by TargetScan miRNA prediction tool **c.** miRNAs reported by miRanda miRNA prediction tool **d.** Venn diagram representing shared miRNAs amongst the three prediction tools. **e.** List of miRNAs that are mutually predicted by miRDB and TargetScan. **f.** List of miRNAs that are mutually predicted by all the three tools.

TargetScanHuman are depicted in Supplementary Fig. 1, 2a respectively. The miRNA prediction scores are displayed in Table 1. Supplementary Fig. 2b presents the target conservation among various species by TargetScan. The miRNAs, reported by only one miRNA prediction tool were removed and ruled out for the further analysis (Fig. 1).

3.3. In silico energy calculations (ΔGhybrid) for the miRNA-mRNA

The miRNAs (11 miRNAs, Fig. 2f) that overlap in the outputs obtained from all the three target prediction tools were finally considered for the further *in silico* analysis, while rest of the miRNAs were dropped off. Afterwards, RNAHybrid tool was employed and determined the negative energies for the opted miRNA-3′UTR Tmprss2 binding pair. Table 1 and Fig.3 reports the values for ΔGhybrid (kcal mol^{-1}) and binding interactions respectively for the selected 11 miRNAs with Tmprss2.

3.4. Secondary structure analysis for the selected miRNAs

The dot-bracket notation of the secondary structures (mature miRNAs and pre-miRNAs) is exhibited in Fig. 4a and b respectively. Besides, estimation for the thermodynamic ensemble, minimum free energy (MFE) in pre-miRNA and mature miRNA is demonstrated in Table 2. Fig. 5 exemplifies the secondary structures for pre-miRNA, mature miRNA, Tmprss2 (3′UTR) and the binding interactions (mature miRNA-Tmprss2) for the selected 11 common miRNAs respectively.

3.5. Identification of miRNA(s) that specifically targets Tmprss2

The resultant miRNAs from the RNAHybrid and RNAfold based analysis were further sorted depending on the accessibility of the target using Sfold web server. Sfold package encompasses various tools for the design and prediction of precise RNA binding partners. STarMir package in the Sfold server attends target accessibility score along with target binding sites on the miRNA, centered on logistic prediction models originating through crosslinking immunoprecipitation studies. The results for the 11 selected miRNAs in the Sfold server are reported in Table 2. The observations ultimately assisted in the assortment of final set of three miRNAs (hsa-miR-214/ miR214, hsa-miR-98/ miR98 and hsa-miR-32-3p/ miR32) having logistic target probability score of more than 0.8. Additionally, the target accessibility probability profiles (for miR214, miR98 and miR32) are shown in the Fig. 6. Supplementary Table 2 depicts the probability profile as per individual nucleotides in the Tmprss2. Furthermore, for the detailed understanding regarding binding energy of mRNA-anti-oligonucleotide and mRNA-siRNA, Soligo and Sirna modules of Sfold software were respectively used. In all cases, the results which represented the best and optimum values are shortlisted and reported in Supplementary Table 3, 4. Therefore, miRNAs *viz.* miR214, miR98 and miR32 were finally selected as best miRNA candidates (*in silico*) showing precise binding with Tmprss2 for the miRNA antagonism based molecular therapies.

3.6. miR214, miR98 and miR32 targets Tmprss2 in vitro

In order to validate the observations from *in silico* analysis, *in vitro* lab validation studies were carried out, primarily with transfections for miR214, miR98 and miR32 in the Caco-2 culture. Successive transfection was affirmed by qPCR based relative abundance of miRNAs (miR214, miR98 and miR32) at 20, 40 and 80 nM concentrations for each of the mentioned miRNAs. Fig. 7a shows an effective transfection of all the three miRNAs at 20, 40 and 80 nM with significantly higher miRNA expression at 40 nM (137.24, 506.07, 881.11 folds) and 80 nM (112.52, 466.47, 767.54 folds) as compared to 20 nM (29.94, 151.55, 257.30 folds) in the mimic treated groups relative to miC and mock control (C).

Further, silencing of Tmprss2 was assessed in the miRNAs transfected wells, results exemplified that these Tmprss2 specific miRNAs can reduce the transcript's expression significantly at 20 nM (miR214, 0.36; miR98, 0.43; miR32, 0.27), 40 nM (miR214, 0.11; miR98, 0.07; miR32, 0.022) and 80 nM (miR214, 0.43 ; miR98, 0.33 ; miR32, 0.14) in comparison to miC and MC (Fig. 7b–d respectively). Additionally, maximum target suppression for Tmprss2 was witnessed in transfections with hsa-miR-32 in contrast to hsa-miR214 and hsa-miR98 at 40 nM.

Interestingly, the studies extended to the protein expression analysis, depicting the miRNA mediated repression in the TMPRSS2 protein on miR32, miR98 and miR214 treatments at 40 nM (Fig. 7e, f). Hence, the

Table 1
miRNA prediction scores with negative energy calculations for selected miRNA-Tmprss2 binding pairs.

S No	miRNA	Features							
		miRanda	miRDB	TargetScan					RNAHybrid
		mirSVR score	Prediction Score	Site type	Context++ score	Context++ score percentile	Weighted context++ score	Conserved branch length	ΔGhybrid/ MFE[a](kcal mol^{-1})
1	**hsa-miR-214**	−0.7068	93	8mer	−0.3	97	−0.1	0.014	−19.2
2	**hsa-miR-98**	−0.6927	93	8mer	−0.35	91	−0.12	1.858	−24.2
3	**hsa-miR-32-3p**	−0.3439	57	7mer-A1	−0.09	95	−0.03	0	−20.9
4	**hsa-let-7a-5p**	−0.6927	93	8mer	−0.35	91	−0.12	1.858	−23.9
5	**hsa-let-7b-5p**	−0.6927	94	8mer	−0.36	92	−0.12	1.858	−29.2
6	**hsa-let-7c-5p**	−0.6927	93	8mer	−0.35	91	−0.12	1.858	−23.9
7	**hsa-let-7d-5p**	−0.7001	93	8mer	−0.35	90	−0.12	1.858	−21.4
8	**hsa-let-7e-5p**	−0.6927	93	8mer	−0.35	91	−0.12	1.858	−21.4
9	**hsa-let-7f-5p**	−0.6927	93	8mer	−0.35	91	−0.12	1.858	−23.9
10	**hsa-let-7 g-5p**	−0.689	93	8mer	−0.35	91	−0.12	1.858	−25.5
11	**hsa-let-7i-5p**	−0.6927	93	8mer	−0.35	91	−0.12	1.858	−25.2

[a] Minimum Free energy.

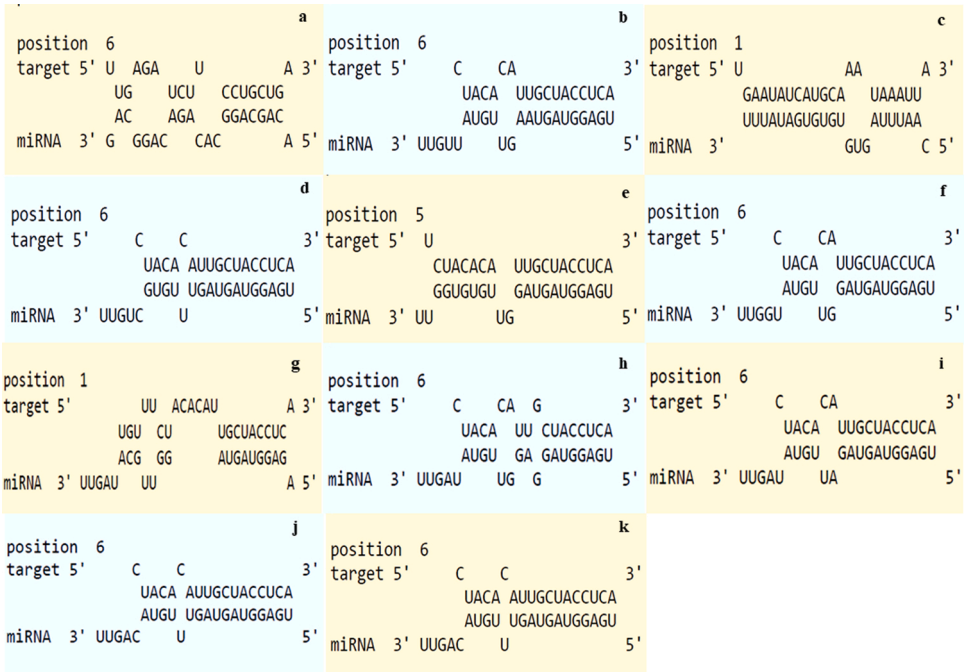

Fig. 3. Analysis of RNAHybrid tool based predictive binding interactions of miRNA-target hybrid. Interacting nucleic acid bases in **a.** miR214 and Tmprss2 **b.** miR98 and Tmprss2 **c.** miR32 and Tmprss2 **d.** hsa-let-7a and Tmprss2. **e.** hsa-let-7b and Tmprss2 **f.** hsa-let-7c and Tmprss2 **g.** hsa-let-7d and Tmprss2 **h.** hsa-let-7e and Tmprss2 **i.** hsa-let-7f and Tmprss2 **j.** hsa-let-7 g and Tmprss2 **k.** hsa-let-7i and Tmprss2, the hybridization of active miRNA binders with the target.

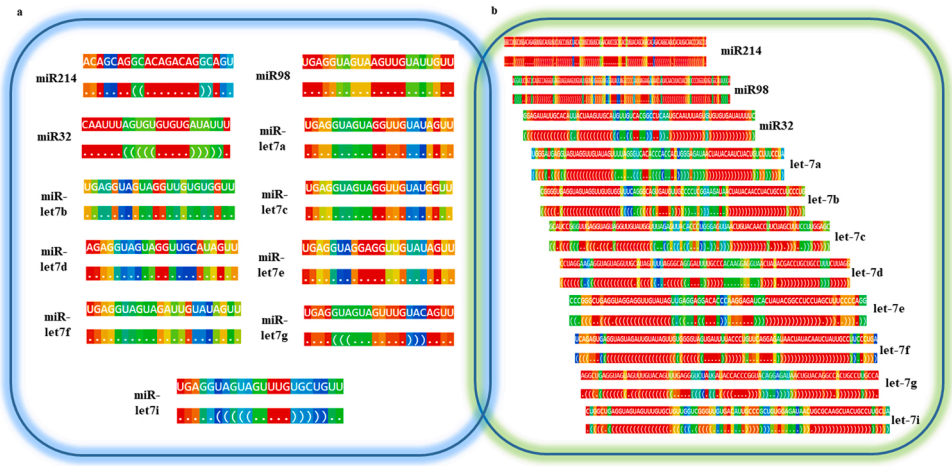

Fig. 4. Illustrations depicting the dot bracket notations **a.** mature miRNAs **b.** precursor miRNAs (pre-miRNA). hsa-let-7a-5p/ let-7a, hsa-let-7b-5p/ let-7b, hsa-let-7c-5p/ let-7c, hsa-let-7d-5p/ let-7d, hsa-let-7e-5p/ let-7e, hsa-let-7f-5p/ let-7f, hsa-let-7 g-5p, let-7 g, hsa-let-7i-5p/let-7i.

findings display the successive suppression of Tmprss2 target by all the three identified potent miRNAs at gene as well as protein level.

4. Discussion

RNA interference makes an innovative next generation tool in the molecular regulation, for targeting the cellular signaling macromolecules associated to biological responses in a disease pathogenesis. In this study, we envisage on miRNA driven molecular therapeutic interventions involving specific targeting of Tmprss2, embarking on the high throughput identification and screening of putative miRNAs. This was facilitated by computational algorithms along with investigational validations, for their mechanistic and functional utility in COVID-19 molecular therapy.

Majority of the current investigational miRNA based drugs are directed against the viral S protein-ACE2 receptor checkpoint (Martinez, 2020). Further, several recent drugs have emerged as beneficial therapeutics in the management of SARS-CoV-2 replication and associated symptoms. Imatinib, Colchicine and N-acetylcysteine showed valuable therapeutic responses in CoV-2 infected case reports. However, their efficacy in COVID-19 management is still in its infancy. Moreover, the case studies based on treatments from Imatinib and Colchicine were uncontrolled and restricted in nature (Della-Torre et al., 2020; Ibrahim et al., 2020; Morales-Ortega et al., 2020). At present, the mainstream therapies are involving aforesaid axis and have proved its significance in the management of CoV-2 replication, but the role of other secondary targets cannot be ruled out in controlling the infection of the virus. Tmprss2, being one such protease, assists in SARS-CoV-2 mediated invasion of the human respiratory system by warranting the viral entry ticket through priming of the CoV-2 spike protein (Lukassen et al.,

Table 2
Web based structural characterization for the selected miRNAs using RNAfold and Sfold tools.

S No	miRNA	Features															
		RNAfold								Sfold							
		Free energy[a](kcal mol^{-1})		Frequency[b](%)		Diversity[c]		Minimum Free energy(kcal mol^{-1})		LogitProb	Seed_Type	ΔGnucl (k cal mol^{-1})	ΔGtotal(k cal mol^{-1})	Site_Access	Seed_Access	Upstream_AU (30 nt)	Dwstream_AU (30 nt)
		Pre miRNA	Mature miRNA	Pre miRNA	Mature miRNA	Pre miRNA	Mature miRNA	Pre miRNA	Mature miRNA								
1	**hsa-miR-214**	−67.5	−1.24	89.13	41.3	0.3	2.11	−67.50	−0.7	0.945	8mer	−7.219	−20.946	0.957	0.954	0.6	1
2	**hsa-miR-98**	−57.87	−0.34	15.02	57.55	5.07	3.01	−56.7	0	0.938	8mer	−7.726	−24.547	0.946	0.99	0.667	1
3	**hsa-miR-32-3p**	−31.45	−0.76	9.48	40.05	5.15	2.71	−30.00	−0.2	0.894	7mer-A1	−5.686	−19.803	0.757	0.91	1	0.933
4	**hsa-let-7a-5p**	−35.18	−0.20	20.37	72.3	5.63	1.51	−34.2	0	0.194	7mer-m8	−0.053	29.931	0.257	0.376	0.267	0.533
5	**hsa-let-7b-5p**	−48.38	−0.04	6.52	94.2	7.6	0.29	−46.7	0	0.22	7mer-m8	−0.054	24.847	0.259	0.379	0.267	0.533
6	**hsa-let-7c-5p**	−33.1	−0.14	6.35	79.8	7.33	1.15	−31.4	0	0.207	7mer-m8	−0.046	27.133	0.258	0.378	0.267	0.533
7	**hsa-let-7d-5p**	−44.51	−0.83	5.34	26.11	5.76	3.12	−42.7	0	0.346	7mer-m8	−0.077	3.36	0.351	0.384	0.3	0.533
8	**hsa-let-7e-5p**	−38.07	−0.14	10.79	79.80	7.09	1.05	−36.7	0	0.269	7mer-m8	−0.073	14.737	0.296	0.376	0.233	0.533
9	**hsa-let-7f-5p**	−41.28	−0.23	39.26	69.32	2.13	1.74	−40.7	0	0.249	7mer-m8	−0.046	18.131	0.294	0.372	0.233	0.533
10	**hsa-let-7 g-5p**	−39.81	−1.07	43.68	39.51	3.44	3.14	−39.3	−0.50	0.312	7mer-m8	−0.107	7.459	0.387	0.38	0.3	0.533
11	**hsa-let-7i-5p**	−40.99	−2.63	12.29	42.02	5.00	4.3	−39.7	−2.1	0.177	7mer-m8	−0.374	30.681	0.318	0.374	0.367	0.533

[a] Free energy of the thermodynamic ensemble (kcal mol^{-1}).
[b] Frequency of the MFE structure (%).
[c] Ensemble diversity.

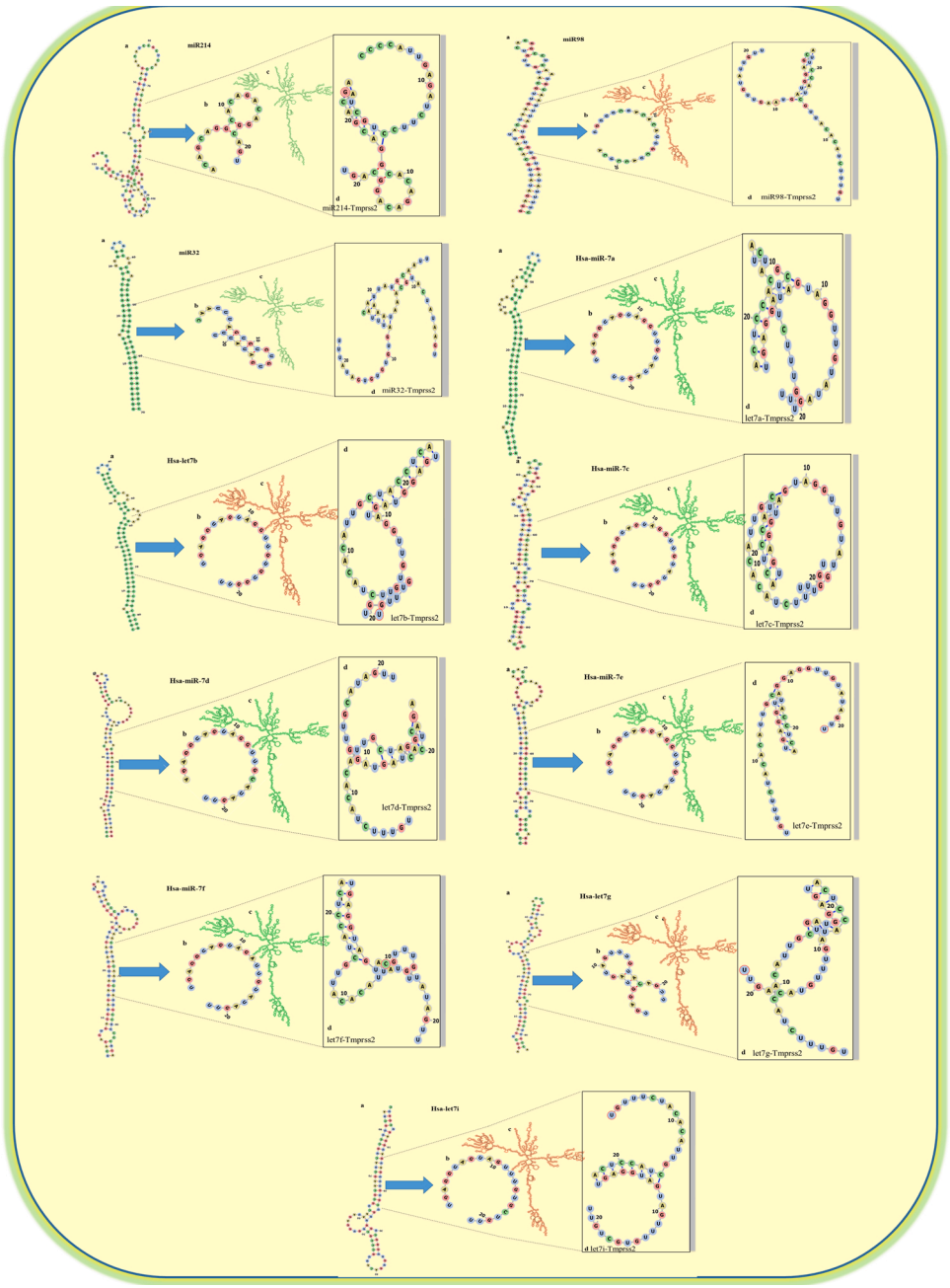

Fig. 5. Target binding and structure modulation assessment through web based RNAfold tool; Secondary structures for **a.** pre-miRNAs **b.** mature miRNA **c.** Tmprss2 (3′UTR) **d.** Interactions of nucleic acid bases of miRNAs and target (Tmprss2), depicting the active binding partners.

2020). Tmprss2, showing evident expression in the human lung's epithelial cells (Donaldson et al., 2002; Paoloni-Giacobino et al., 1997), holds fine capability of degrading S protein chiefly at S1/S2 and the S2′ locations of the viral proteins further permitting fusion of the membranes (Hoffmann et al., 2020). Apart from, alveolar cells (type 2) and bronchial cells, Tmprss2 depicted expression across various tissues, *viz.* prostate, colon, kidney, breasts *etc.* (Stopsack et al., 2020). In addition, studies in the past years have reported, Tmprss2 partaking in the pathogenesis and diagnosis of the prostate cancer (Hossain and Bostwick, 2013; Zoni et al., 2018). Considering Tmprss2 as a critical drug target, we advocated, miR214, miR98 and miR32 to be employed as potential therapeutics in the specific suppression of the Tmprss2. Seenprachawong et al., have designed a computational pipeline for upstream target identification of specific miRNAs with its mechanistic utility in the osteo-signaling, and regulation for bone related injuries (Seenprachawong et al., 2016). Our study, exploits the existing *in silico* pipeline with improvisation to identify warrior miRNAs against CoV-2. Recent studies have reported about the potential usage of miRNAs against various genome targets of CoV-2, hsa-miR-4661-3p have been shown targeting S protein (Zhi Liu et al., 2020). Whereas, MR147-3p (viral miRNA) stimulates Tmprss2 expression with resultant upregulation of CoV-2 function in the gut (Zhi Liu et al., 2020). On contrary, the present study, reports the host miRNAs targeting Tmprss2, a strategy involving lesser possibilities of harmful side effects. The scheme mentioned in Fig. 1, enabled us with identification of 3 potential miRNAs having high affinity for Tmprss2. We considered three different *in silico* tools (TargetScanHuman 7.2, miRanda and miRDB) for the initial scanning of miRNAs against the transcript for Tmprss2. TargetScan forecasts the predicted miRNA targets basis seed region (conserved sequence that is generally positioned at locations 2–7 from the 5′end of

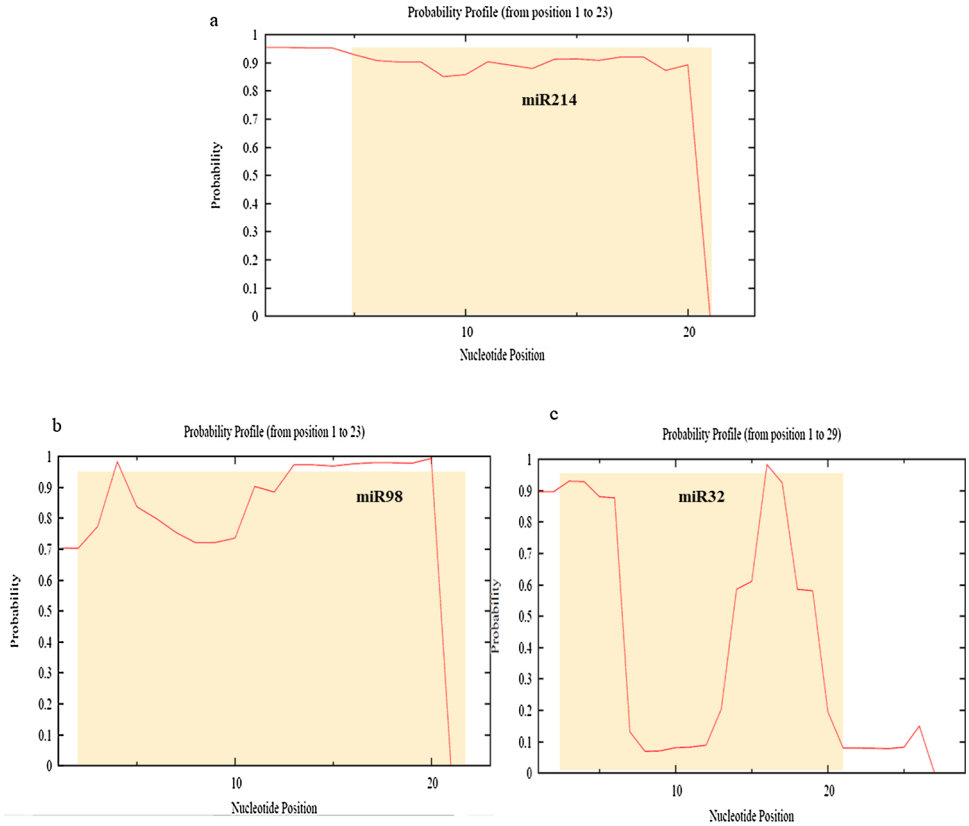

Fig. 6. Probability scores and specific target accessibility with respect to Tmprss2 mRNA for the three enriched miRNAs (miR214, miR98 and miR32). Output binding region (yellow) has been represented as histogram. Higher probability scores signifies the stronger binding probability of miRNA to the target (Tmprss2).

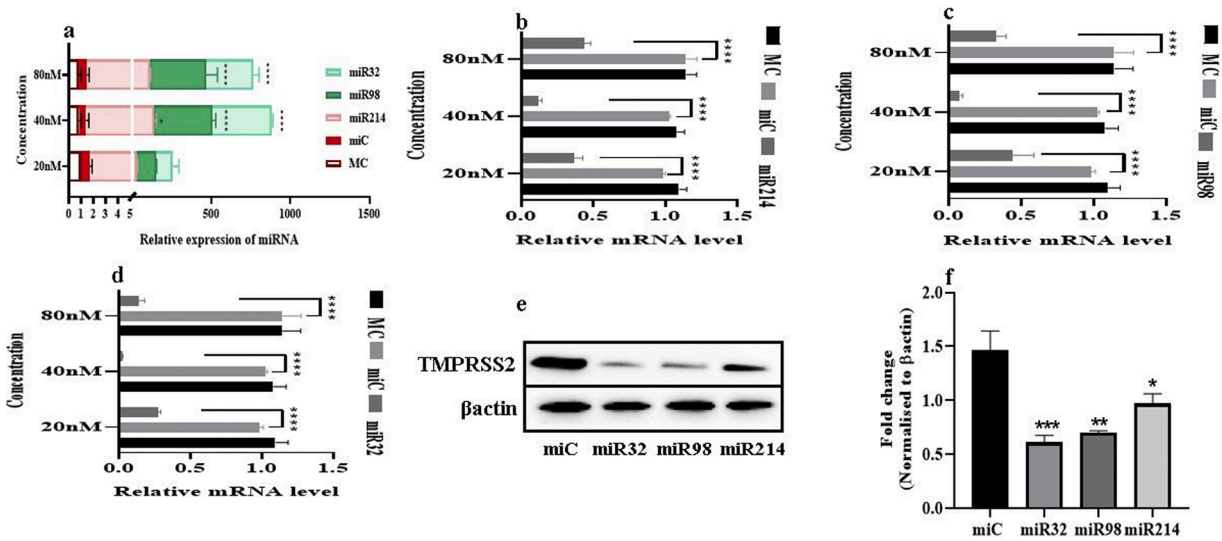

Fig. 7. *In vitro* target validation for Tmprss2 in hsa-miR214, hsa-miR98 and hsa-miR-32. **a.** Caco-2 were transfected with miC (negative control), miR214, miR98 and miR32 at 20, 40, 80 nM followed by determination of effective transfection by qPCR. **b.** Experimental investigation for Tmprss2 as validated target in hsa-miR214. Caco-2 cells were transfected with miC, miR214 and assessed for Tmprss2 gene expression at 20, 40 and 80 nM by qPCR. **c.** Experimental investigation for Tmprss2 as validated target in hsa-miR98. Caco-2 cells were transfected with miC, miR98 and assessed for Tmprss2 gene expression at 20, 40 and 80 nM by qPCR. **d.** Experimental investigation for Tmprss2 as validated target in hsa-miR32. Caco-2 cells were transfected with miC, miR32 and assessed for Tmprss2 gene expression at 20, 40 and 80 nM by qPCR. **e, f.** Experimental investigation for TMPRSS2 protein as validated target in miR32, miR98 and miR214 at 40 nM. **MC** Mock Control, contains transfecting Opti-MEM media with RNAiMAX transfecting reagent only. All values represent means ± S.E. (n = 3). *P < 0.05, ***P < 0.001, ****P < 0.0001 compared with the miC.

miRNA) matches in mRNA-miRNA in mammals, flies, worms, and fish. Further, it examines phylogeny while predicting the conservation of UTRs among different species (Dweep et al., 2013). miRDB, recognizes the putative miRNAs and targets using machine learning, SVM classifier in human, mouse, rat, dog and chicken (Dweep et al., 2013). Albeit, miRanda adopts two chief rules, sequence match with wobble pairing

and conservation of mRNA transcripts in the related species, emphasizing multiple binding sites in a miRNA (Dweep et al., 2013). The conceptual basis for selecting foresaid tools was encompassing comprehensive criteria for the prediction of various miRNAs and targets. Subsequently, 11 miRNAs were sorted from a pool of 123 miRNAs, basis selection of mutual miRNAs reported from all the three tools. For the further scrutinisation, negative energy calculations were executed for the 11 selected miRNA and 3′UTR Tmprss2 using RNAHybrid tool, which energetically aligns the shorter sequence of the miRNA along the best fit mRNA sequences (Ishida and Selaru, 2013). Besides, RNAfold web server, providing the specific binding region in the miRNA sequence gives clear picture and indication for the precise binding between the 11 miRNAs-Tmprss2 with high negative ΔGhybrid values. RNAfold anticipates the optimal secondary structure for DNA or RNA input sequences, designs strands folding to a fixed query secondary structure and examines that the combinatorial set of DNA and RNA input possess least undesirable secondary structure. Further it provides a predictive minimum free energy estimate along with base pair probabilities for the query sequences (maximum input length 10,000 nucleotides) resulting to a user friendly output file (PS, SVG) (Bestle et al., 2020). Finally in order to select the specific miRNAs among the previous list, Sfold server was taken into consideration that incorporates various tools for the design and prediction of precise RNA binding partners (Rennie et al., 2014). STarMir module of the Sfold web server provides miRNA binding sites on the target. The probability score in the Sfold output represents the confidence measure for the prediction of the accurate site, a score of 0.5 or higher reflects satisfactory binding possibility for the miRNA (Ding et al., 2004; Rennie et al., 2014). The miRNA with probability profiles greater than 0.8 were therefore selected as specific binders for the Tmprss2 resulting in its possible suppression with exalted binding efficiency. miR214, miR98 and miR32 were finally obtained as robust interactors, post screening from a repertoire of 123 miRNAs. Furthermore, the three *in silico* screened miRNAs binders were experimentally validated through gene and protein expressions in the Caco-2 cells. The high expression of Tmprss2 in Caco-2 cells has been associated previously which facilitates the SARS-CoV-2 entry efficiently, with an advantage for investigation of therapeutic modalities (Hoffmann et al., 2020). miR214, miR98 and miR32 significantly suppressed Tmprss2 transcript at 20, 40 and 80 nM and TMPRSS2 protein at 40 nM of their concentrations individually, with highest gene repression observed in miR32, corroborating an effective gene silencing approach for the check of Tmprss2 mediated viral entry in the host.

Expression of miR214 was downregulated due to acute murine coronavirus infection in oligodendrocytes with an associated inhibitory response on the target genes (Zhang and Cao, 2015). Additionally, gene silencing through miR214 in case of accessory viral infections such as vesiculovirus and hepatitis C replications, supports as crucial molecular interventions for therapy (Iizuka et al., 2012; Zhang et al., 2017). Albeit, overexpression of miR214 has been noticed as host defensive in the SARS-HCoV contaminated bronchoalveolar stem cells (Leon-Icaza et al., 2019), verifying our observations with *in vitro* assays, however, further extensive investigational validations will be required for comprehensive understanding of mechanistic role, in the account of miR214 upregulation or specific delivery having an inhibitory effect on CoV-2 replication. In addition, studies in the recent past have demonstrated decreased expression for miR98 in the West Nile virus infected brains (Kumar and Nerurkar, 2014). Interestingly, miR98 has been acknowledged with an established role in the pathogenesis of SARS-CoV, assisting in the viral transmission and replication through stimulated differentiation of bronchoalveolar stem cells with downregulated ACE2 (Mallick et al., 2009). Moreover, earlier studies indicated for the viral (SARS-CoV) nucleocapsid mediated downregulation for miR98, influencing viral entry in the alveolar cells (Leon-Icaza et al., 2019). Likewise, Sardar et al., have lately informed, hsa-miR98 targeting the Spike protein in SARS-CoV-2 genome with an associated expression for Hepatitis C virus (Sardar et al., 2020). Besides, Rota and Gallagher et al., have also demonstrated the prominence of miR98 dependent targeting of S protein in SARS-CoV (Gallagher and Buchmeier, 2001; Rota et al., 2003). In the context of miR32, studies have documented the direct inhibition of RNA virus, primate foamy retrovirus type 1 (comparable to HIV1) at the protein level with supplementary degradative function in the coding region for influenza PB1 (Trobaugh and Klimstra, 2017). Moreover, miR-32 has been reported with a significant regulatory role in avian hepatitis A viral infections (Wu et al., 2020). Recently, regulations through miR98 and miR214 expression in CoVs-infected hosts has been sporadically demonstrated, subsequently, are in concordance to the observations from the current study (Leon-Icaza et al., 2019). While, in our study under explored miR32 have comparatively shown a promising therapeutic efficacy, for the management of CoV-2 infections. In addition, viral intervention targeting Tmprss2 has been demonstrated in several studies from recent reports in the mouse models as well as human cell lines with knockdown of Tmprss2 exhibiting a reduced viral invasion (Bestle et al., 2020; Glowacka et al., 2011; Iwata-Yoshikawa et al., 2019; Stopsack et al., 2020; Strope et al., 2020). Tmprss2 has shown additional involvement in the activation of several extracellular matrix associated substrates in certain cancers (Satyam et al., 2020). Studies have informed the stimulating actions on matriptase from Tmprss2 facilitating prostate cancer growth and progression. Additionally, Tmprss2 supports cellular migration in the breast cancer while targeting ECM components (Ko et al., 2015). Therefore, miRNA mediated specific suppression of Tmprss2 would also be beneficial tool in the control of other disorders. In conjugation with the findings in the present investigations, these miRNA may appropriate to be employed for designing therapeutic modalities against COVID-19, hence, represents their promising action for the Bio-drugs development.

5. Conclusion

Conventional strategies for drug discovery demand not only huge capital but also consumes ample time, which restricts the detailed analysis and generation of effective remedial modalities. Next generation *in silico* methodologies, are rapid, providing insights in the mechanistic action of the novel drugs. In the scenario of COVID-19 pandemic with short turnover time, speedy identification of therapeutic targets, holds paramount importance. Targeting at the entry step, depicts an upper edge over the other strategies, controlling late viral replication phases. Therefore, our study, employing computational pipeline and lab validation, recognizes hsa-miR-214, hsa-miR-98 and hsa-miR-32 with a prospective therapeutic character for silencing Tmprss2. These three miRNAs showed strong binding affinity against Tmprss2 (which assist in the viral entry) with highest probability scores of interaction, especially the miR32 which was comparatively observed best *in vitro* for its inhibitory effect. Since, miRNAs display promiscuous traits, consequently, resulting in off-target effects. Hence their overexpression in tissue specific supply (*via.* nanoparticle) could potentially regulate or inhibit the associated process of viral entry. However, further detailed *in vivo* validations are needed for the ultimate mechanistic functionalities along with the comprehensive understanding of CoV-2 pathogenesis.

Funding

None.

Animal and human ethics

No animals/humans were used for studies that are base of this research.

Author's contributions

TK executed the work plan and wrote the manuscript, SK (Suman), RK, SK (Sandeep), DU assisted in the drafting, revision and supervision

of the manuscript, MK provided support with *in silico* tools and CS gave the concept and design of the study.

Declaration of Competing Interest

The authors declare that they have no conflict of interest in the publication

Acknowledgement

None

Appendix A. Supplementary data

Supplementary material related to this article can be found, in the online version, at doi:https://doi.org/10.1016/j.virusres.2020.198275.

References

Bandiera, S., Pfeffer, S., Baumert, T.F., Zeisel, M.B., 2015. miR-122–a key factor and therapeutic target in liver disease. J. Hepatol. 62, 448–457.
Bestle, D., Heindl, M.R., Limburg, H., Van Lam van, T., Pilgram, O., Moulton, H., Stein, D. A., Hardes, K., Eickmann, M., Dolnik, O., Rohde, C., Klenk, H.D., Garten, W., Steinmetzer, T., Bottcher-Friebertshauser, E., 2020. TMPRSS2 and furin are both essential for proteolytic activation of SARS-CoV-2 in human airway cells. Life Sci. Alliance 3.
Bittmann, S., Moschuring Alieva, E., Weissenstein, A., Luchter, E., Villalon, G., 2020. The role of TMPRSS2-Inhibitor camostat in the pathogenesis of COVID-19 in lung cells. Stem Cell Res. 1, 1–3.
Della-Torre, E., Della-Torre, F., Kusanovic, M., Scotti, R., Ramirez, G.A., Dagna, L., Tresoldi, M., 2020. Treating COVID-19 with colchicine in community healthcare setting. Clin. Immunol. 217, 108490.
Ding, Y., Chan, C.Y., Lawrence, C.E., 2004. Sfold web server for statistical folding and rational design of nucleic acids. Nucleic Acids Res. 32, W135–141.
Donaldson, S.H., Hirsh, A., Li, D.C., Holloway, G., Chao, J., Boucher, R.C., Gabriel, S.E., 2002. Regulation of the epithelial sodium channel by serine proteases in human airways. J. Biol. Chem. 277, 8338–8345.
Dweep, H., Sticht, C., Gretz, N., 2013. In-silico algorithms for the screening of possible microRNA binding sites and their interactions. Curr. Genomics 14, 127–136.
Filipowicz, W., Bhattacharyya, S.N., Sonenberg, N., 2008. Mechanisms of post-transcriptional regulation by microRNAs: are the answers in sight? Nat. Rev. Genet. 9, 102–114.
Gallagher, T.M., Buchmeier, M.J., 2001. Coronavirus spike proteins in viral entry and pathogenesis. Virology 279, 371–374.
Glowacka, I., Bertram, S., Muller, M.A., Allen, P., Soilleux, E., Pfefferle, S., Steffen, I., Tsegaye, T.S., He, Y., Gnirss, K., Niemeyer, D., Schneider, H., Drosten, C., Pohlmann, S., 2011. Evidence that TMPRSS2 activates the severe acute respiratory syndrome coronavirus spike protein for membrane fusion and reduces viral control by the humoral immune response. J. Virol. 85, 4122–4134.
Gu, S., Jin, L., Zhang, F., Sarnow, P., Kay, M.A., 2009. Biological basis for restriction of microRNA targets to the 3' untranslated region in mammalian mRNAs. Nat. Struct. Mol. Biol. 16, 144–150.
Hoffmann, M., Kleine-Weber, H., Schroeder, S., Kruger, N., Herrler, T., Erichsen, S., Schiergens, T.S., Herrler, G., Wu, N.H., Nitsche, A., Muller, M.A., Drosten, C., Pohlmann, S., 2020. SARS-CoV-2 cell entry depends on ACE2 and TMPRSS2 and is blocked by a clinically proven protease inhibitor. Cell 181 (271–280), e278.
Hossain, D., Bostwick, D.G., 2013. Significance of the TMPRSS2:ERG gene fusion in prostate cancer. BJU Int. 111, 834–835.
Ibrahim, H., Perl, A., Smith, D., Lewis, T., Kon, Z., Goldenberg, R., Yarta, K., Staniloae, C., Williams, M., 2020. Therapeutic blockade of inflammation in severe COVID-19 infection with intravenous N-acetylcysteine. Clin. Immunol. 219, 108544.
Iizuka, M., Ogawa, T., Enomoto, M., Motoyama, H., Yoshizato, K., Ikeda, K., Kawada, N., 2012. Induction of microRNA-214-5p in human and rodent liver fibrosis. Fibrogenesis Tissue Repair 5, 12.
Ishida, M., Selaru, F.M., 2013. miRNA-based therapeutic strategies. Curr. Anesthesiol. Rep. 1, 63–70.
Iwata-Yoshikawa, N., Okamura, T., Shimizu, Y., Hasegawa, H., Takeda, M., Nagata, N., 2019. TMPRSS2 contributes to virus spread and immunopathology in the airways of murine models after coronavirus infection. J. Virol. 93.
John, A.A., Prakash, R., Kureel, J., Singh, D., 2018. Identification of novel microRNA inhibiting actin cytoskeletal rearrangement thereby suppressing osteoblast differentiation. J. Mol. Med. 96, 427–444.
Kaur, T., John, A.A., Sharma, C., Vashisht, N.K., Singh, D., Kapila, R., Kapila, S., 2020. miR300 intervenes Smad3/β-catenin/RunX2 crosstalk for therapy with an alternate function as indicative biomarker in osteoporosis. Bone, 115603.
Ko, C.J., Huang, C.C., Lin, H.Y., Juan, C.P., Lan, S.W., Shyu, H.Y., Wu, S.R., Hsiao, P.W., Huang, H.P., Shun, C.T., Lee, M.S., 2015. Androgen-induced TMPRSS2 activates matriptase and promotes extracellular matrix degradation, prostate cancer cell invasion, tumor growth, and metastasis. Cancer Res. 75, 2949–2960.
Kuhn, N., Bergmann, S., Kosterke, N., Lambertz, R.L.O., Keppner, A., van den Brand, J.M. A., Pohlmann, S., Weiss, S., Hummler, E., Hatesuer, B., Schughart, K., 2016. The proteolytic activation of (H3N2) influenza a virus hemagglutinin is facilitated by different type II transmembrane serine proteases. J. Virol. 90, 4298–4307.
Kumar, M., Nerurkar, V.R., 2014. Integrated analysis of microRNAs and their disease related targets in the brain of mice infected with West Nile virus. Virology 452-453, 143–151.
Leon-Icaza, S.A., Zeng, M., Rosas-Taraco, A.G., 2019. microRNAs in viral acute respiratory infections: immune regulation, biomarkers, therapy, and vaccines. ExRNA 1.
Lukassen, S., Chua, R.L., Trefzer, T., Kahn, N.C., Schneider, M.A., Muley, T., Winter, H., Meister, M., Veith, C., Boots, A.W., Hennig, B.P., Kreuter, M., Conrad, C., Eils, R., 2020. SARS-CoV-2 receptor ACE2 and TMPRSS2 are primarily expressed in bronchial transient secretory cells. EMBO J. 39, e105114.
Mallick, B., Ghosh, Z., Chakrabarti, J., 2009. MicroRNome analysis unravels the molecular basis of SARS infection in bronchoalveolar stem cells. PLoS One 4, e7837.
Martinez, M.A., 2020. Compounds with therapeutic potential against novel respiratory 2019 coronavirus. Antimicrob. Agents Chemother. 64.
Matsuyama, S., Nagata, N., Shirato, K., Kawase, M., Takeda, M., Taguchi, F., 2010. Efficient activation of the severe acute respiratory syndrome coronavirus spike protein by the transmembrane protease TMPRSS2. J. Virol. 84, 12658–12664.
Morales-Ortega, A., Bernal-Bello, D., Llarena-Barroso, C., Frutos-Perez, B., Duarte-Millan, M.A., Garcia de Viedma-Garcia, V., Farfan-Sedano, A.I., Canalejo-Castrillero, E., Ruiz-Giardin, J.M., Ruiz-Ruiz, J., San Martin-Lopez, J.V., 2020. Imatinib for COVID-19: a case report. Clin. Immunol. 218, 108518.
Paoloni-Giacobino, A., Chen, H., Peitsch, M.C., Rossier, C., Antonarakis, S.E., 1997. Cloning of the TMPRSS2 gene, which encodes a novel serine protease with transmembrane, LDLRA, and SRCR domains and maps to 21q22.3. Genomics 44, 309–320.
Peterson, S.M., Thompson, J.A., Ufkin, M.L., Sathyanarayana, P., Liaw, L., Congdon, C.B., 2014. Common features of microRNA target prediction tools. Front. Genet. 5, 23.
Rehmsmeier, M., Steffen, P., Hochsmann, M., Giegerich, R., 2004. Fast and effective prediction of microRNA/target duplexes. RNA 10, 1507–1517.
Rennie, W., Liu, C., Carmack, C.S., Wolenc, A., Kanoria, S., Lu, J., Long, D., Ding, Y., 2014. STarMir: a web server for prediction of microRNA binding sites. Nucleic Acids Res. 42, W114–118.
Rota, P.A., Oberste, M.S., Monroe, S.S., Nix, W.A., Campagnoli, R., Icenogle, J.P., Penaranda, S., Bankamp, B., Maher, K., Chen, M.H., Tong, S., Tamin, A., Lowe, L., Frace, M., DeRisi, J.L., Chen, Q., Wang, D., Erdman, D.D., Peret, T.C., Burns, C., Ksiazek, T.G., Rollin, P.E., Sanchez, A., Liffick, S., Holloway, B., Limor, J., McCaustland, K., Olsen-Rasmussen, M., Fouchier, R., Gunther, S., Osterhaus, A.D., Drosten, C., Pallansch, M.A., Anderson, L.J., Bellini, W.J., 2003. Characterization of a novel coronavirus associated with severe acute respiratory syndrome. Science 300, 1394–1399.
Sardar, R., Satish, D., Birla, S., Gupta, D., 2020. Comparative analyses of SAR-CoV2 genomes from different geographical locations and other coronavirus family genomes reveals unique features potentially consequential to host-virus interaction and pathogenesis. bioRxiv.
Satyam, A., Tsokos, M.G., Tresback, J.S., Zeugolis, D.I., Tsokos, G.C., 2020. Cell-derived extracellular matrix-rich biomimetic substrate supports podocyte proliferation, differentiation, and maintenance of native phenotype. Adv. Funct. Mater. 30, 1908752.
Seenprachawong, K., Nuchnoi, P., Nantasenamat, C., Prachayasittikul, V., Supokawej, A., 2016. Computational identification of miRNAs that modulate the differentiation of mesenchymal stem cells to osteoblasts. PeerJ 4, e1976.
Shirogane, Y., Takeda, M., Iwasaki, M., Ishiguro, N., Takeuchi, H., Nakatsu, Y., Tahara, M., Kikuta, H., Yanagi, Y., 2008. Efficient multiplication of human metapneumovirus in Vero cells expressing the transmembrane serine protease TMPRSS2. J. Virol. 82, 8942–8946.
Stopsack, K.H., Mucci, L.A., Antonarakis, E.S., Nelson, P.S., Kantoff, P.W., 2020. TMPRSS2 and COVID-19: Serendipity or Opportunity for Intervention? Cancer Discov. 10, 779–782.
Strope, J.D., Pharm, D.C., Figg, W.D., 2020. TMPRSS2: potential biomarker for COVID-19 outcomes. J. Clin. Pharmacol. 60, 801–807.
Tarnow, C., Engels, G., Arendt, A., Schwalm, F., Sediri, H., Preuss, A., Nelson, P.S., Garten, W., Klenk, H.D., Gabriel, G., Bottcher-Friebertshauser, E., 2014. TMPRSS2 is a host factor that is essential for pneumotropism and pathogenicity of H7N9 influenza A virus in mice. J. Virol. 88, 4744–4751.
Trobaugh, D.W., Klimstra, W.B., 2017. MicroRNA regulation of RNA virus replication and pathogenesis. Trends Mol. Med. 23, 80–93.
Uno, Y., 2020. Camostat mesilate therapy for COVID-19. Intern. Emerg. Med.
Verdecchia, P., Cavallini, C., Spanevello, A., Angeli, F., 2020. The pivotal link between ACE2 deficiency and SARS-CoV-2 infection. Eur. J. Intern. Med. 76, 14–20.
Wu, F., Lu, F., Fan, X., Chao, J., Liu, C., Pan, Q., Sun, H., Zhang, X., 2020. Immune-related miRNA-mRNA regulation network in the livers of DHAV-3-infected ducklings. BMC Genomics 21, 123.
Zhang, X.Y.L., Cao, Jianzhong, 2015. Regulation of cellular MicroRNA expression in oligodendrocytes during acute and persistent coronavirus infection. Virol. Mycol. 4, 8.
Zhang, C., Yi, L., Feng, S., Liu, X., Su, J., Lin, L., Tu, J., 2017. MicroRNA miR-214 inhibits snakehead vesiculovirus replication by targeting the coding regions of viral N and P. J. Gen. Virol. 98, 1611–1619.
Zhi Liu, J.W., Yuyu, Xu, Guo, Mengchen, Mi, Kai, Xu, Rui, Pei, Yang, Zhang, Qiangkun, Luan, Xiaoting, Hu, Zhibin, Liu, Xingyin, 2020. Implications of the virus-encoded

miRNA and host miRNA in the pathogenicity of SARS-CoV-2. arXiv preprint arXiv, 2004.04874.

Zhou, P., Yang, X.L., Wang, X.G., Hu, B., Zhang, L., Zhang, W., Si, H.R., Zhu, Y., Li, B., Huang, C.L., Chen, H.D., Chen, J., Luo, Y., Guo, H., Jiang, R.D., Liu, M.Q., Chen, Y., Shen, X.R., Wang, X., Zheng, X.S., Zhao, K., Chen, Q.J., Deng, F., Liu, L.L., Yan, B., Zhan, F.X., Wang, Y.Y., Xiao, G.F., Shi, Z.L., 2020. A pneumonia outbreak associated with a new coronavirus of probable bat origin. Nature 579, 270–273.

Zoni, E., Karkampouna, S., Thalmann, G.N., Kruithof-de Julio, M., Spahn, M., 2018. Emerging aspects of microRNA interaction with TMPRSS2-ERG and endocrine therapy. Mol. Cell. Endocrinol. 462, 9–16.